ELSEVIER

Surface Science 482–485 (2001) 300–305

SURFACE SCIENCE

www.elsevier.nl/locate/susc

Surface characterization of new non-toxic titanium alloys for use as biomaterials

M.F. López [a,*], A. Gutiérrez [b], J.A. Jiménez [a]

[a] *Dep. Ingeniería de Materiales, Degradación y Durabilidad, Centro Nacional de Investigaciones Metalúrgicas, CSIC, Avda Gregorio del Amo 8, E-28040 Madrid, Spain*

[b] *Departamento de Ciencia y Tecnología de Materiales, Universidad Miguel Hernández, Avda Ferrocarril s/n, E-03202 Elche, Spain*

Abstract

The surface oxide layers formed spontaneously through air contact on three new, non-toxic titanium alloys have been investigated by X-ray photoelectron spectroscopy (XPS). The alloys investigated were Ti–7Nb–6Al, Ti–13Nb–13Zr and Ti–15Zr–4Nb. The results show a large surface enrichment in Al oxides and Zr oxides, respectively, which indicates a considerable outwards diffusion of these two elements. However, an analysis of the Nb 3d spectra reveals that the formation of Nb oxides at the surface is less favoured than in the case of the other alloying elements. The XPS data show for all three Ti alloys a passive layer formed by a mixture of Ti, Al or Zr and Nb oxides. © 2001 Elsevier Science B.V. All rights reserved.

Keywords: X-ray photoelectron spectroscopy; Corrosion; Oxidation; Alloys; Polycrystalline surfaces

1. Introduction

Corrosion of metallic biomaterials is a twofold problem. On the one side, it leads to material degradation. On the other side, it produces ion release with harmful effects on the organism. The presence or absence of a protective surface oxide film controls the corrosion behaviour of materials. Corrosion resistant materials react easily with oxygen from the atmosphere giving rise to a surface oxide layer, the so-called passive layer, which acts as a barrier against further oxidation [1–4].

Amongst conventional biomaterials, pure Ti as well as Ti–6Al–4V alloy exhibit excellent properties for surgical implant applications [5,6]. The excellent corrosion resistance of pure Ti is attributed to the formation of a TiO_2 protective layer on its surface. By adding alloying elements to titanium, such as Al and V, its mechanical properties are improved [7–9]. However, for a better biocompatibility it seems important to avoid in the composition the presence of V due to the toxic effects of V ion release [10]. Zr, Al, Nb, Ta and Pt are possible alloying elements that exhibit excellent biocompatibility, belonging to the non-toxic group in tissue interaction. Therefore, for applications in biomedicine it is crucial the development of new Ti alloys with good mechanical properties but with no V content. A detailed determination

* Corresponding author. Tel.: +34-915538900/+34-966658408; fax: +34-915347425.

E-mail address: paquil@cenim.csic.es (M.F. López).

PII: S0039-6028(00)01005-0

of the surface composition is essential in the development of new biomaterials because the most external layers will be in direct contact with the biological tissues. Besides, as mentioned above, the corrosion behaviour of a material is directly controlled by the composition of its passive layer.

The aim of this work is to perform a comparative surface characterization of the passive layer of three new titanium alloys not containing V developed for biomedical applications. The choice of the alloying elements in titanium alloys will lead to α-, (α + β)- or β-alloys. (α + β)-titanium alloys provide higher strength than pure titanium with similar corrosion resistance. The group of (α + β)-alloys includes the most common titanium alloy: Ti–6Al–4V. With the aim of finding a substitute to this alloy without V in its composition, three (α + β)-alloys were studied: Ti–7Nb–6Al, Ti–13Nb–13Zr and Ti–15Zr–4Nb. The comparative surface characterization of these Ti alloys was performed by means of X-ray photoelectron spectroscopy (XPS). The XPS results show differences in the chemical composition of the Ti alloys surface layers, suggesting differences in their protective character.

2. Experimental

Three Ti basis alloys were prepared by arc melting and then casting in a cooper coquille under high vacuum. The chemical composition of these alloys were (in wt.%): Ti–7Nb–6Al, Ti–13Nb–13Zr and Ti–15Zr–4Nb. In order to obtain a lamellar (α + β) microstructure, which ensures satisfactory mechanical properties, the same annealing procedure was followed on all samples. The alloys were heat treated above the β-transition temperature at 1100°C for 1 h and subsequently aged at 700°C for 1 h. Before testing, the samples were mechanically polished with SiC emery paper up to #600, and then ultrasonically degreased in acetone.

The composition of the passive layer of the different materials was studied by XPS. XPS spectra were recorded under ultra-high vacuum (UHV) conditions with a VG-CLAM hemispherical electron energy analyser using Mg X-rays as excitation source. The base pressure in the UHV chamber during measurements was better than 10^{-9} mbar. Samples were cleaned by sputtering with an ion gun operating with a sample current of 1 μA, an ion energy of 5 keV and a sputter rate of approximately 10 Å min^{-1}.

3. Results and discussion

Fig. 1 shows the surface atomic composition of all three samples, Ti–7Nb–6Al, Ti–13Nb–13Zr and Ti–15Zr–4Nb, as determined by XPS. The values represented in this graph include for each element all oxidation states. This figure reveals the important role of Al and Zr, which are present at the surface at elevated rates. On the other hand, the amount of Nb at the surface is quite low. The reason to select Nb as one of the alloying elements is its capability to stabilize the β-phase. Al is an α-stabilizing element while zirconium is highly soluble in both phases. The addition of a β-stabilizer plus an adequate thermal treatment makes possible the presence of both phases, leading to excellent mechanical properties. Consequently, although the presence of Nb is essential

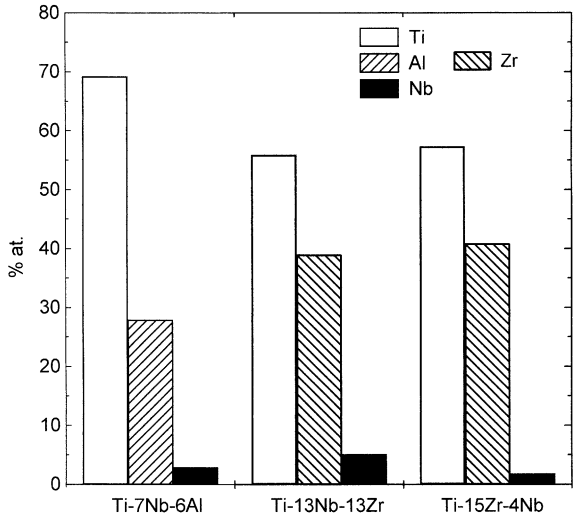

Fig. 1. Atomic percentage of the main alloying elements at the surface of the three different Ti alloys, as obtained from the XPS spectra.

Table 1
Atomic percentage of the main alloying element of all three samples at the surface, the corresponding value in the bulk, and the ratio between both

Material	Alloying element	Surface (at.%)	Bulk (at.%)	Ratio surface/bulk
Ti–7Nb–6Al	Al	27.9	10.5	2.65
Ti–13Nb–13Zr	Zr	39	7.8	5.01
Ti–15Zr–4Nb	Zr	40.9	8.6	4.73

in the bulk, Fig. 1 shows that its contribution to the surface properties is not significant.

It is interesting to normalize the atomic composition at the surface with that at the bulk in order to estimate the actual outwards diffusion of the alloying elements. Table 1 shows the atomic percentage of the main alloying element of all three samples at the surface, the corresponding value in the bulk, and the ratio between both. This ratio gives an estimation of the surface enrichment originated by the diffusion process. As can be observed, the Al content at the surface of Ti–7Nb–6Al is almost three times that in the bulk, whereas in the case of Zr, both in Zr in Ti–13Nb–13Zr and Ti–15Zr–4Nb, the ratio surface/bulk is even higher.

A deeper analysis should have into account the oxidation state of the different elements. To perform this analysis, the XPS spectra were least-squares fitted using standard Gaussian–Lorentzian lines and the corresponding integral background. As an example, the results of such fitting procedure on the Ti-2p spectra of the Ti–13Nb–13Zr alloy after three different sputtering times are shown in Fig. 2. The first sputtering cycle, 30 s, was carried out to clean the surface. Depth profiling was performed at two additional sputtering times for this sample. The solid lines through the data points represent the result of the least-squares fit, with an additional solid curve representing the integral background. Four doublets were used to simulate the possible Ti oxidation states, i.e., Ti^0, Ti^{2+}, Ti^{3+} and Ti^{4+}. For each oxidation state, the width and position were fixed, and only the intensity was allowed to vary freely, leading to different values as a function of the sputtering time. Binding energies at 454.3, 455.7, 457.7 and 459.3 eV correspond to Ti^0, Ti^{2+}, Ti^{3+} and Ti^{4+} $2p_{3/2}$

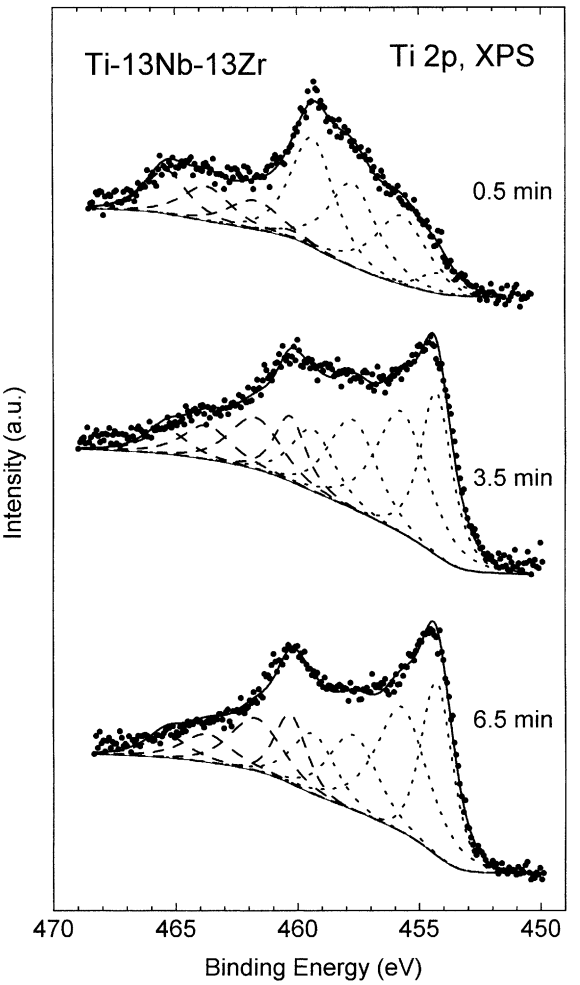

Fig. 2. Ti 2p XPS spectra of Ti–13Nb–13Zr alloy after three different sputtering times. The dotted subspectra represent the $2p_{3/2}$ emissions for Ti^0, Ti^{2+}, Ti^{3+} and Ti^{4+}, and the dashed subspectra the corresponding $2p_{1/2}$ emissions.

emission respectively. The spin orbit splitting was 6.0 eV. The same fitting procedure was followed for the different XPS spectra of all samples. In order to obtain quantitative results from the XPS analysis, both the intensity of the different emission peaks and the atomic sensitivity factors of the different elements were taken into account. In the fitting analysis, each oxidation state is represented by a Gaussian–Lorentzian curve. For each element, the area of every Gaussian–Lorentzian curve, i.e., of every oxidation state was calculated.

All these values were normalized using the atomic sensitivity factors for the corresponding element. Finally, taking into account the normalized areas, the atomic percentages of the oxidation states for all the different elements were calculated.

The fitting analyses were performed after depth profiling at different sputtering times: 30 s, 3.5, 6.5, and 14.5 min. As it was explained above for Ti, the XPS fitting analysis leads to four different oxidation states: Ti^0, Ti^{2+}, Ti^{3+} and Ti^{4+}. For Nb the fitting procedure gives rise to the following oxidation states: Nb^0, Nb^{2+}, Nb^{4+} and Nb^{5+}. For Zr the oxidation states obtained were Zr^0, Zr^{3+} and Zr^{4+}. For the case of Al, Al^0 and Al^{3+} were observed. It is known that ion bombardment produces reduction of metal oxides by means of preferential sputtering of the oxygen atoms. The contribution due to the effect of ion bombardment on the different intermediate oxidation states is probably smaller than the contribution due to the actual presence of these oxidation states in the passive layer. However, in order to avoid wrong interpretations of the XPS analysis results, only the metallic (zero oxidation state) and the highest oxidation state components will be represented.

Figs. 3–5 show the results of the depth profiles performed on Ti–7Nb–6Al, Ti–13Nb–13Zr and Ti–15Zr–4Nb, respectively, taking into account the different elements and the possible oxidation states. However, in these figures are represented only the metallic and the highest oxidation state components. Fig. 3 corresponds to Ti–7Nb–6Al, and shows the evolution of the different elements for four different sputtering times: 30 s, 3.5, 6.5, and 14.5 min. All metallic components (zero oxidation state) increase as a function of sputtering time, as it is expected. In the case of aluminium the oxidized component decreases gradually with sputtering time, with the largest amount of Al^{3+} at the surface. For titanium and niobium, however the behaviour is different, probably due to the presence of more chemical species. The highest oxidation states of Ti and Nb, Ti^{4+} and Nb^{5+}, decrease after the first sputtering cycle abruptly. This effect is related to the maximum contribution of the highest oxidation states, Ti^{4+} and Nb^{5+}, at the surface. Figs. 4 and 5 show the behaviour of the different Zr, Ti and Nb oxidation states as a function of sputtering times for Ti–13Nb–13Zr and Ti–15Nb–4Zr. Although the chemical composition is different to the previous case, these two alloys show similar trends. The metallic component contribution of the different elements increases with sputtering time. The highest oxidation

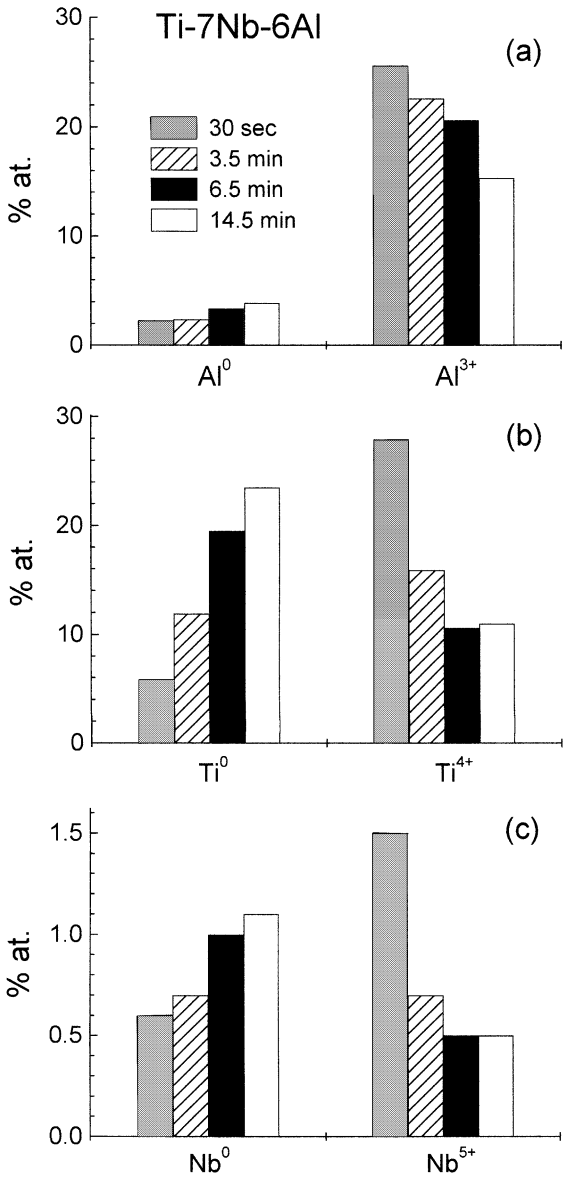

Fig. 3. Atomic percentage as a function of the sputtering time for Ti–7Nb–6Al alloy of (a) Al^0 and Al^{3+}, (b) Ti^0 and Ti^{4+}, and (c) Nb^0 and Nb^{5+}.

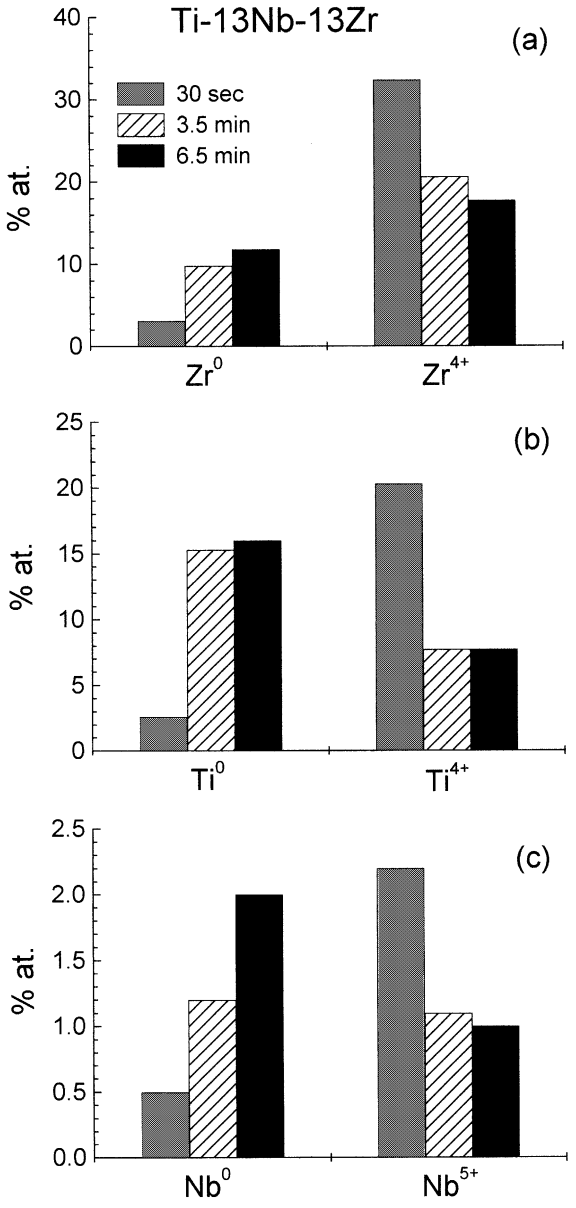

Fig. 4. Atomic percentage as a function of the sputtering time for Ti–13Nb–13Zr alloy of (a) Zr^0 and Zr^{4+}, (b) Ti^0 and Ti^{4+}, and (c) Nb^0 and Nb^{5+}.

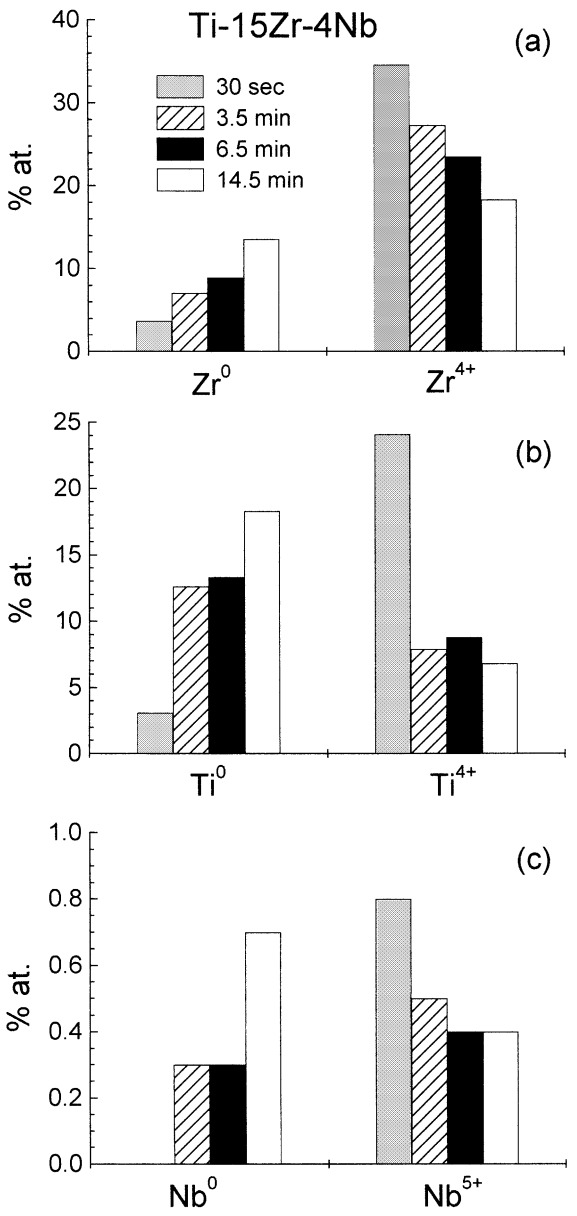

Fig. 5. Atomic percentage as a function of the sputtering time for Ti–15Zr–4Nb alloy of (a) Zr^0 and Zr^{4+}, (b) Ti^0 and Ti^{4+}, and (c) Nb^0 and Nb^{5+}.

states decrease abruptly after the first sputtering cycle. As it was mentioned above, for the case of Al in the Ti–7Nb–6Al sample, Al^0 and Al^{3+} were observed. In contrast to this result, the presence of Zr in Ti–13Nb–13Zr and Ti–15Nb–4Zr make possible the existence of an intermediate oxidation state for this element. These results obtained in Figs. 3–5 together with the observation of intermediate oxidation states confirm the expected complexity of the passive layer composition. The

XPS data reveal that the topmost of the surface contains the higher percentage of the highest oxidation states. The metallic components are observed in a higher proportion at the deeper region of the passive layer. It is important to point out the low contribution of Nb oxides at the surface, as it was already observed in Fig. 1, with the highest Nb contribution for the Ti–13Zr–13Nb sample, where the highest percentage of Nb in the bulk composition is also found. The results obtained from the XPS data indicate that for these alloys the passive layer is formed by a mixture of Ti, Al or Zr, and, in lower proportion, Nb oxides.

4. Conclusions

The passive layer of three new titanium alloys not containing V developed for biomedical applications has been investigated by XPS. A large enhancement of the α-stabilizing element (Al for Ti–7Nb–6Al, and Zr for Ti–13Nb–13Zr and Ti–15Nb–4Zr) is observed at the outermost surface. In order to obtain information on the different chemical states, and their depth evolution, XPS spectra for several sputtering times were performed on all samples. The results show a clear diffusion of Zr and Al from bulk to the surface to form oxides while Nb is less favoured. The passive layer of the three new Ti alloys is formed by a mixture of Ti, Al or Zr, and, in less proportion, Nb oxides.

Acknowledgements

The authors are gratefully acknowledged to Prof. G. Fommeyer from Max-Planck Institut für Eisenforschung (Düsseldorf) for kindly supplying the Ti alloys specimens. This work has been supported by the project 07N-0050-1999 of the Spanish "Programa de Tecnología de los Materiales de la Comunidad Autónoma de Madrid".

References

[1] D.A. Jones, Principles and Prevention of Corrosion, second ed., Prentice Hall, Upper Saddle River, NJ, 1996.
[2] D. Talbot, J. Talbot, Corrosion Science and Technology, CRC Press, Boston, 1998.
[3] M.F. López, A. Gutiérrez, M.C. García-Alonso, M.L. Escudero, Solid State Commun. 101 (1997) 575.
[4] M.F. López, M.L. Escudero, E. Vida, A.R. Pierna, Electrochim. Acta 42 (1997) 659.
[5] D.H. Kohn, P. Ducheyne, in: D.F. Williams (Ed.), Medical and Dental Materials. Serie Materials Science and Technology, vol. 14, Weinheim, 1992, p. 29.
[6] H.J. Breme, V. Biehl, J.A. Helsen, in: J.A. Helsen, H.J. Breme (Eds.), Metals as Biomaterials, Wiley, Chichester, 1998, p. 40.
[7] R. Boyer, G. Welsch, E.E. Collings, Materials Properties Handbook: Titanium Alloys, ASM, Metals Park, OH, 1994.
[8] G. Lutjering, Mat. Sci. Eng. A 263 (1999) 117.
[9] C. Bathias, K. El Alami, T.Y. Wu, Eng. Fract. Mech. 56 (1997) 255.
[10] Y. Okazaki, S. Rao, Y. Ito, T. Tateishi, Biomaterials 19 (1998) 1197.